CASE 65

Wiper System Chatter Reduction

Abstract: The wiper arm/blade forms an integral part of a windshield wiper system. *Chatter* occurs when the wiper blade does not take the proper set and "skips" across the windshield during operation, causing both acoustic and wipe quality deterioration, which significantly affects customer satisfaction. Instead of measuring wiper quality deterioration, a robust design approach was used by evaluating the actual time that a blade takes to reach a fixed point on the windshield at a given cycle. That means that the focus was on measuring the functionality of the system and not the end characteristics. Nine control factors were used under all categories of noise factors. Eighteen design configurations were tested in this study.

1. Introduction

Windshield Wiper System

A windshield wiper system is composed of four major subsystems: (1) the wiper motor, (2) the wiper linkage assembly, (3) the pivot towers, and (4) the wiper arm/blade combination. The wiper motor provides driving power to the system. The wiper linkage assembly (usually, a series- or parallel-coupled four-bar mechanism) is a mechanical transmission configuration to transfer the driving power from the motor to the pivots and to change the rotary motion of the motor to an oscillating motion at the pivots. The pivot towers provide a firm anchor from which the pivots operate, holding the wiper pivots in proper orientation with the windshield surface. When the arm/blade combinations are attached to the pivot and the system is cycled, the blades clear two arc-shaped wipe patterns on the windshield.

The customer expectations for a good windshield wiper system are:

- ❑ Clear vision under a wide variety of operating conditions
- ❑ Multiple levels of wiper speed
- ❑ Uniform wiper pattern
- ❑ Quiet under all weather conditions
- ❑ Long life and high reliability

Definition of Chatter

Chatter occurs when a wiper blade does not take the proper set and skips across the windshield during operation, causing both acoustic and wipe quality deterioration, which significantly affect customer satisfaction. From the results of previous studies it was determined that the components that contribute most to chatter are the arms and blades. This study was conducted to understand more thoroughly the specific design factors relating to arm/blade combinations that affect system performance.

2. Description of the Experiment

Engineered System

Control and noise factors were selected based on knowledge of chatter. The engineered system is shown in Figure 1.

Ideal Function

The ideal function for this study was based on the following hypothesis: For an ideal system, the actual

 Taguchi's Quality Engineering Handbook. Genichi Taguchi, Subir Chowdhury and Yuin Wu

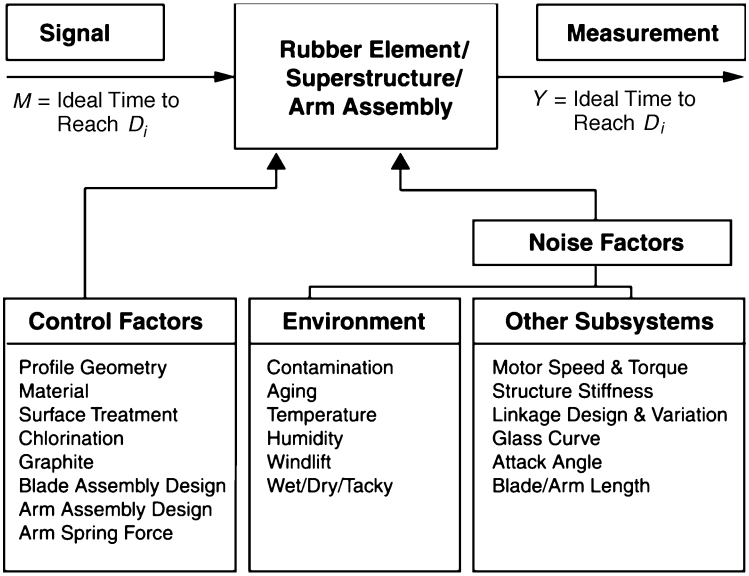

Figure 1
Engineered system

time for the wiper blades to reach a fixed point on the windshield during a cycle should be the same as the theoretical time (ideal time) for which the system was designed. Under the presence of the noise factors, the actual time will differ from the theoretical time. Furthermore, the actual time of a robust system under varying noise conditions should have less variation and be closer to the theoretical time. Therefore, the system ideal function is given by

$$Y_i = \beta M_i$$

where Y_i is the actual time it takes the blade to reach a fixed point on the windshield at the ith cycle, M_i the theoretical time for the blade to reach a fixed point on the windshield at the ith cycle, and $\beta = i/$ motor rpm. The ideal system function is shown in Figure 2.

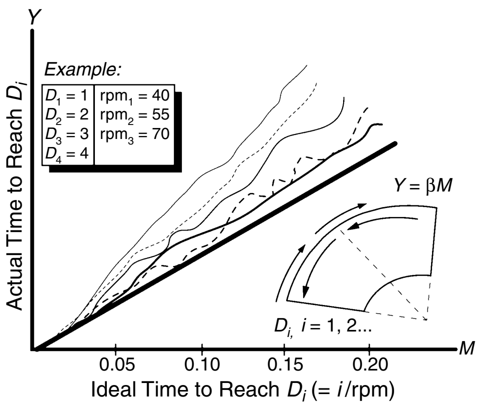

Figure 2
Ideal function

Three rpm values were used in the experiment: 40, 55, and 70. In general, due to the noise effects, the actual time would always be longer than the theoretical time determined by the design (i.e., $b > 1$, and $b = 1$ would be the ideal case).

In this experiment, other measurements were also observed: (1) the lateral load on the wiper arm and (2) the normal load on the wiper arm.

Noise Strategy

In general, noises can be categorized as follows:

1. Piece-to-piece variation (manufacturer, material variation, etc).
2. Change in dimension due to wear, fatigue, and so on

3. Customer use/duty cycle
4. External environment (climate, road, wind, temperature, etc).
5. Internal environment (interface with other body systems)

In this experiment, the important noise factors were grouped into two noise factors, each with two levels: (1) Noise factor S included factors such as wiper angular orientation in park position, temperature, humidity, and condition of blades, which would produce a tendency to ac variability (i.e., variation about the mean response time):

$S_1 = -30$ at park/200°C/50% humidity/before aging

$S_2 = 10$ at park/20°C/90% humidity/after aging

(2) Noise factor T is the windshield surface condition, wet or dry, that would produce a tendency to dc variability in the response time (i.e., shifting the mean):

$$T_1 = \text{wet surface condition}$$

$$T_2 = \text{dry surface condition}$$

The Control Factors

The control factors and their levels (Table 1) were selected through team brainstorming.

3. Experimental Results and Data Analysis

Design of Experiment

The L_{18} orthogonal array shown in Table 2 was selected for the design of experiment. It may be seen that under each run there are 12 tests at different rpm's and combined noise conditions.

Test Setup

A special test fixture was built for this experiment, and three sensors were attached to the windshield to record a signal when a wiper blade passes them. Strain gauges were attached to the wiper arm for continuous recording of lateral and normal loads to the wiper arm. Typical testing results are shown in Figure 3.

Test Results

In this study, only the analysis of time measurement data is presented. Under each test, the system was run for a certain period of operating time, and the actual accumulated operating times for the blade to pass a fixed point were recorded against the ideal operating time, determined by the nominal rpm setting of the constant-rpm motor. A testing data plot for this measurement is shown in Figure 4.

The regression analyses were conducted for those data and the slopes of the regression lines

Table 1
Control factors and levels

Control Factor	Level 1	Level 2	Level 3
A: arm lateral rigidity design	1	2	3
B: superstructure rigidity	Median	High	Low
C: vertebra shape	Straight	Concave	Convex
D: spring force	Low	High	—
E: profile geometry	1	2	New design
F: rubber material	I	II	III
G: graphite	Current	Higher graphite	None
H: chlorination	Median	High	Low
I: attachment method	Current clip	Modified	Twin screw

Table 2
Design of experiment

	Factor									rpm 1				rpm 2				rpm 3			
										S_1		S_2		S_1		S_2		S_1		S_2	
Run	*D*	*A*	*B*	*C*	*E*	*F*	*G*	*H*	*I*	Wet	Dry	Wet	Dry	Wet	Dry	Wet	Dry	Wet	Dry	Wet	Dry
1	1	1	1	1	1	1	1	1	1												
2	1	1	2	2	2	2	2	2	1												
3	1	1	3	3	3	3	3	3	1												
4	1	2	1	1	2	2	3	3	2												
5	1	2	2	2	3	3	1	1	2												
6	1	2	3	3	1	1	2	2	2												
7	1	3	1	2	1	3	2	3	3												
8	1	3	2	3	2	1	3	1	3												
9	1	3	3	1	3	2	1	2	3												
10	2	1	2	3	3	2	2	1	2												
11	2	1	2	1	1	3	3	2	2												
12	2	1	3	2	2	1	1	3	2												
13	2	2	1	2	3	1	3	2	3												
14	2	2	2	3	1	2	1	3	3												
15	2	2	3	1	2	3	2	1	3												
16	2	3	1	3	2	3	1	2	1												
17	2	3	2	1	3	1	2	3	1												
18	2	3	3	2	1	2	3	1	1												

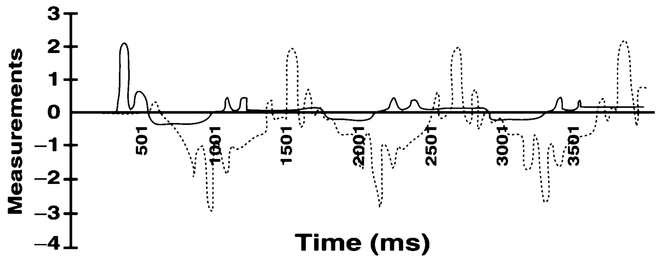

Figure 3
Plot of a typical testing data

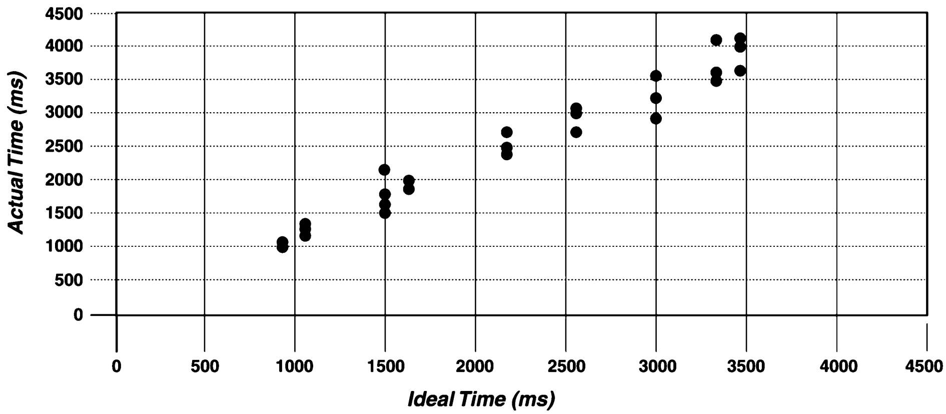

Figure 4
Typical testing data plot

Table 3
SN ratio and β value for each run

Run	*D*	Factor *A*	*B*	*C*	*E*	*F*	*G*	*H*	*I*	SN	β
1	Low	Design 1	Median	Straight	Geo 1	Material I	Current	Median	Current	−34.27	1.078
2	Low	Design 1	High	concave	Geo 2	Material II	Higher	High	Current	−34.41	1.089
3	Low	Design 2	Low	Convex	New	Material III	None	Low	Current	−44.27	1.133
4	Low	Design 2	Median	Straight	Geo 2	Material II	None	Low	Modified	−37.27	1.096
5	Low	Design 3	High	Concave	New	Material III	Current	Median	Modified	−30.81	1.073
6	Low	Design 3	Low	Convex	Geo 1	Material I	Higher	High	Modified	−32.80	1.093
7	Low	Design 3	Median	Concave	Geo 1	Material III	Higher	Low	Twin screw	−34.65	1.076
8	low	Design 3	High	Convex	Geo 2	Material I	None	Median	Twin screw	−38.89	1.094
9	Low	Design 3	Low	Straight	New	Material II	Current	High	Twin screw	−33.39	1.65
10	High	Design 1	Median	Convex	New	Material II	Higher	Median	Modified	−30.46	1.063
11	High	Design 1	High	Straight	Geo 1	Material III	None	High	Modified	−35.24	1.079
12	High	Design 1	Low	Concave	Geo 2	Material I	Current	Low	Modified	−42.59	1.096
13	High	Design 2	Median	Concave	New	Material I	None	High	Twin screw	−30.54	1.075
14	High	Design 2	High	Convex	Geo 1	Material II	Current	Low	Twin screw	−32.52	1.068
15	High	Design 2	Low	Straight	Geo 2	Material III	Higher	Median	Twin screw	−32.70	1.065
16	High	Design 3	Median	Convex	Geo 2	Material III	Current	High	Current	−31.00	1.065
17	High	Design 3	High	Straight	New	Material I	Higher	Low	Current	−33.67	1.075
18	High	Design 3	Low	Concave	Geo 1	Material II	None	Median	Current	−34.18	1.079

were estimated; the mean square was used to estimate the variation. In Table 3, the SN ratio and β values are evaluated by

$$\text{SN ratio} = 10 \log_{10} \frac{\beta^2}{\sigma^2}$$

where β is the slope of regression line (forced through zero) and σ is the square root of the mean-squared deviation.

4. Data Analysis and the Optimal Condition

The SN ratios and β values given in the last two columns of Table 3 were analyzed further to determine the significance of the control factors and to select the best levels.

SN Ratio

A plot of the SN ratio against the control factors and their levels is shown in Figure 5. From the plot it can be seen that different levels of arm rigidity, superstructure rigidity, graphite, and chlorination yield quite different results, whereas load distribution has a relatively small effect on the SN ratio.

Beta Value

From Figure 6 it may be observed that in contrast to the plot of the SN ratio, where the differences in the impact of the control factor levels are large, differences in the impact of the control factor levels on the β value are relatively small.

Optimal Condition

The optimal condition was determined using two-step optimization, in which selection of the control factor combination was carried out by (1) maximizing the SN ratio and (2) having a β value close to 1.00.

Since the objective was to have minimum variability in motion and minimum difference between actual and theoretical times for the wiper blades to reach a fixed point on the windshield in each cycle, maximizing the SN ratio was the top priority.

Table 4 gives the optimal condition and baseline design. The values predicted for the SN ratio and for β are also shown in Table 4. It may be seen that the SN ratio of the optimal condition has an approximate 10-dB increase over the baseline.

The predicted values shown in Table 4 were calculated as follows.

SN ratio of optimal

$$\begin{aligned}
&= -[34.647 + (32.77 - 34.647) \\
&\quad + (33.03 - 34.647) + (34.42 - 34.647) \\
&\quad + (33.66 - 34.647) + (33.86 - 34.647) \\
&\quad + (33.70 - 34.647) + (33.11 - 34.647) \\
&\quad + (33.55 - 34.647) + (33.78 - 34.647)] \\
&= -24.71
\end{aligned}$$

SN ratio of baseline

$$\begin{aligned}
&= -\,[34.647 + (36.87 - 34.647) \\
&\quad + (33.03 - 34.647) + (34.42 - 34.647) \\
&\quad + (35.64 - 34.647) + (33.94 - 34.647) \\
&\quad + (35.46 - 34.647) + (34.10 - 34.647) \\
&\quad + (33.55 - 34.647) + (35.30 - 34.647)] \\
&= -35.13
\end{aligned}$$

β value of optimal

$$\begin{aligned}
&= [1.08249 + (1.0783 - 1.08249) \\
&\quad + (1.0792 - 1.08249) + (1.0763 - 1.08249) \\
&\quad + (1.0765 - 1.08249) + (1.0807 \;\; 1.08249) \\
&\quad + (1.0767 - 1.08249) + (\text{l.U768} - 1.08249) \\
&\quad + (1.0752 - 1.08249) + (1.0737 - 1.08249)] \\
&= 1.033
\end{aligned}$$

β value of baseline

$$\begin{aligned}
&= [1.08249 + (1.0898 - 1.08249) \\
&\quad + (1.0792 - 1.08249) + (1.0763 - 1.08249) \\
&\quad + (1.0885 - 1.08249) + (1.0788 - 1.08249) \\
&\quad + (1.0852 - 1.08249) + (1.0780 - 1.08249) \\
&\quad + (1.0752 - 1.08249) + (1.0904 - 1.08249)] \\
&= 1.082
\end{aligned}$$

5. Confirmation Tests and Results

The confirmation test plan is as follows:

Baseline configuration: $A_1B_1C_1D_1E_1F_1G_1H_1I_1$

Optimal configuration: $A_2B_1C_1D_2E_3F_2G_2H_2I_3$

See Table 5.

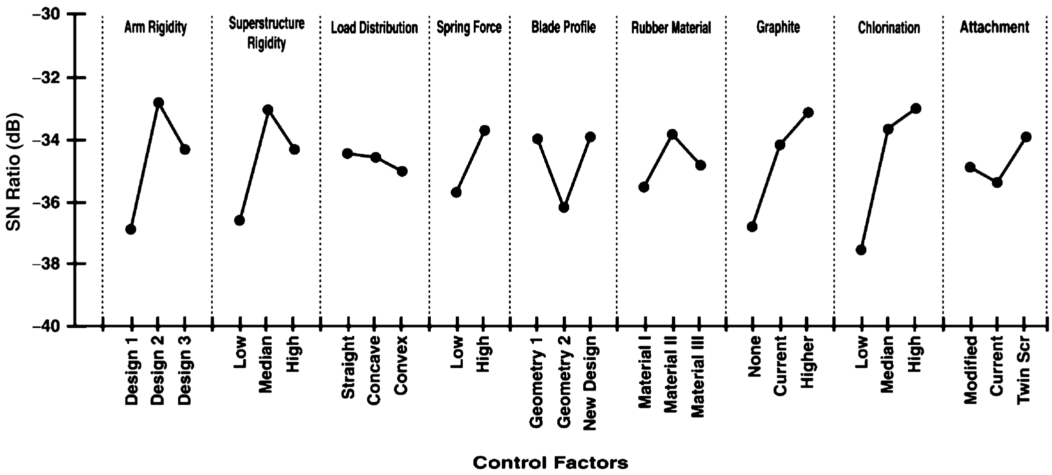

Figure 5
SN ratio chart

6. Conclusions

This robust design study for a windshield wiper system indicates that the chlorination, graphite, arm rigidity, and superstructure rigidity have significant impacts on the optimal wiper system. Load distribution on the blade has a minimal influence. As a result, low friction and high rigidity of the wiper arm and blade will lead to a more robust windshield wiper system.

Acknowledgments The authors wish to thank John King, John Coleman, Dr. Ken Morman, Henry Kopickpo, and Mark Garaseia of Ford Motor Company,

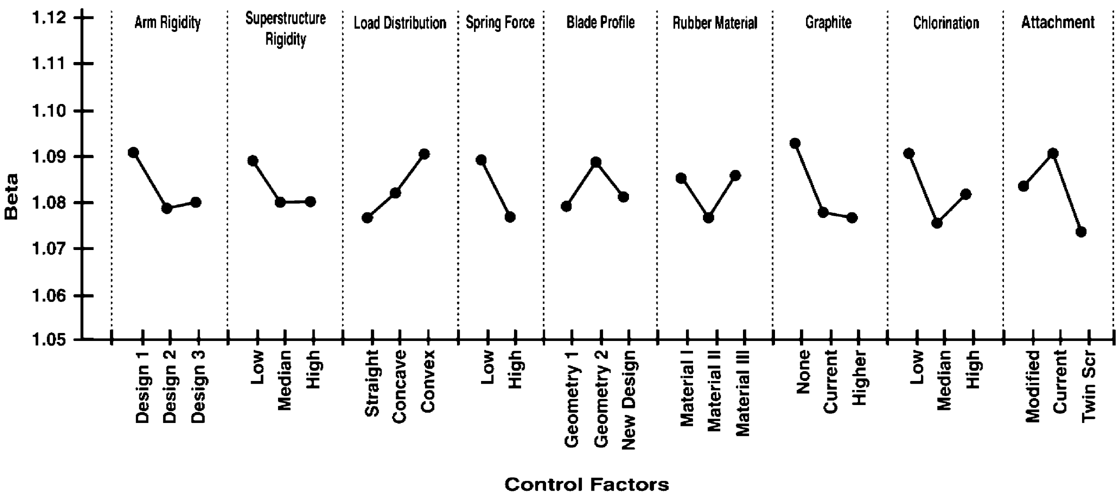

Figure 6
β value chart

Table 4
Optimal conditions and prediction

	Arm Rigidity	Super-structure	Load Distribution	Spring Force	Blade Profile	Rubber Material	Graphite	Chlorination	Attachment	SN	β
Optimal	Design 2	Median	Straight	High	New design	Material 2	Higher	Median	Twin screw	−24.71	1.033
Baseline	Design 1	Median	Straight	Low	Geo 1	Material 1	Current	Median	Current	−35.13	1.082

Table 5
Confirmation test results

	Predicted		Confirmed	
Condition	**SN Ratio**	**β**	**SN Ratio**	**β**
Optimal	−24.71	1.033	−25.41	1.011
Baseline	−35.13	1.082	−36.81	1.01
Gain	10.42	—	11.4	—

and Brian Thomas and Don Hutter for their support during the course of this work.

This case study is contributed by Michael Deng, Dingjun Li, and Wesley Szpunar.